Proceedings of IMECE2007
2007 ASME International Mechanical Engineering Congress and Exposition
November 11-15, 2007, Seattle, Washington, USA

IMECE2007-43549

NEW COMMAND SHAPING METHODS FOR REDUCED VIBRATION OF A SUSPENDED PAYLOAD WITH CONSTRAINED TROLLEY MOTION

Aaron R. Enes, George Woodruff School of Mechanical Engineering, Georgia Institute of Technology, USA

Timothy Y. Hsu, George Woodruff School of Mechanical Engineering, Georgia Institute of Technology, USA

Angela A. Sodemann, George Woodruff School of Mechanical Engineering, Georgia Institute of Technology, USA

ABSTRACT

In manufacturing environments, a common task is to quickly move a suspended payload point-to-point along a fixed overhead conveyor track without inducing significant payload vibration. Recent research in command shaping has shown remarkably effective ways to reduce the swing of a suspended payload providing the motion of the trolley is not constrained. However, the development of a command shaper where the trajectory of the trolley is constrained to follow a fixed curvilinear path has not been explored. This paper will present the development of a simple feedforward command shaper for fast, low vibration, point-to-point movement of a payload suspended from a trolley constrained to follow a fixed generalized path.

The command shaping method involves modifying the command signal by convolving it with a series of impulses. Prior work has suggested command shaping to be very effective for fast, low-vibration movement of flexible systems. In this paper, command shaping methods are applied to an overhead conveyor system constrained to move along a fixed curvilinear path. Two new command shapers are presented for canceling payload vibration induced by motion of the trolley along the path. The designed Tangential Vibration (TV) shaper reduces payload vibrations induced by tangential accelerations of the trolley along the path, while the Centripetal-Tangential Vibration (CTV) shaper reduces vibrations induced by both tangential and centripetal accelerations. A key result of this study is that a command shaper having at least three impulses is required to yield zero residual vibration for motion along a curvilinear path. A simple pendulum payload attached to an actual small-scale overhead trolley following a constrained path is used to evaluate the performance of the designed command shapers. It is shown that the designed shapers significantly reduce payload swing compared to unshaped performance. An experimental sensitivity analysis shows the designed shapers are robust to system modeling errors and variations in path parameters.

INTRODUCTION

The area of crane control has been heavily researched since the 1960s. A recent paper of Abdel-Rahman, et al. [1] reviews the history of crane control techniques. Both open-loop and closed-loop control schemes have been used with success. A brief review of crane control will be presented in this section.

Command shaping, optimal control, closed loop linear control, adaptive control, fuzzy logic control, and nonlinear control have all been applied to the area of crane control research. Lee [2] researched use of sliding surfaces in conjunction with a PID controller. Lew and Khalil [3], on the other hand, developed a linear feedback control method for robotic crane control. Additionally, Yi et al. [4] proposed a fuzzy control using Single Input Rule Modules. These controllers have been shown to be effective in simulations and in implementation.

Command shaping is a technique that has been shown to effectively reduce vibration in a system. In this method, the command signal is pre-filtered. The filtered input signal is the result of a convolution between a command shaper and the original input signal. Typically [5-14], a command shaper consists of a series of impulses. The time between impulses is calculated using a model of the system. In crane applications, the necessary elements for the model are the natural frequency and the damping of the system.

Command shaping has been an active area of continuing research in crane control. Command shaping began with Smith [5] in 1957 with his *Posicast* technique. A major paper in the development of command shaping was authored by Singer and Seering [6]. They showed the cancellation of vibration at an endpoint, the time penalty incurred, and the robustness of a preshaped command with the Draper

Laboratory's Space Shuttle Remote Manipulator System simulator. More recent papers such as Garrido et al [7], have shown the practicality, simplicity, and effectiveness of command shaping. Singhose et al. [8] developed a vector diagram approach to designing command shapers. A United States Patent of Yun et al. [9] also explores the area of command shaping showing velocity profiles and corresponding swing angles. Another Singer et al. [10] paper looks further into different types of input shaping control for cranes. A comprehensive general tutorial on command shaping, with discussions of ZV, ZVD, UMZV, and EI shapers, was written by Singh and Singhose [11]. These command shapers have been shown to effectively cancel out the payload vibration induced during straight line motion.

Lawrence [12] also raises the question if command shaping can reduce swinging in tower cranes. Nonlinearities such as centripetal and Coriolis accelerations complicate the problem. Additionally, tower cranes generate a two dimensional tracking problem, whereas the previously designed shapers were intended for one-dimensional use. In 1996, Singhose et al. [13] successfully used the ZV, UMZV, and EI shapers in two-dimensional tracking problems. Singhose et al. were able to choose a desired path for the payload such as a square and track the path closely using the aforementioned shapers. Blackburn et al. [14] extended this two-dimensional problem to a tower crane motion. He developed a radially assisted command shaper for a tower crane model. However, in the development of all of these works, the trolley path was not constrained.

The research presented in this paper aims to constrain the curved path of the overhead crane trolley and to eliminate the payload swing at a final stopping point. In this research, the trolley path is not allowed to deviate from the defined path. An example of this type of system would be an assembly line in which an overhead rail system transports supplies from one station to another. The tracks are permanent and cannot be altered. Radial assistance is not an option since the path has been set. This research explores how a system constrained this way can achieve minimal vibration at a specified stopping location by using the theories of command shaping.

This paper will present a crane model, develop two command shapers that cancel out vibrations induced by tangential acceleration (TV shaper) and centripetal and tangential accelerations (CTV shaper), and present experimental results demonstrating the use of these shapers. It is assumed in this paper that the crane trolley is fixed in a track and is not allowed to deviate from this path.

The results of implementing the TV and CTV shapers on a model crane, and also the results of an experimental sensitivity analysis of the shapers performed on the model crane will be presented. Discussions and conclusions are presented last.

DERIVATION OF CRANE EQUATIONS OF MOTION FOR COMMAND SHAPING

In this section, the crane is modeled as a three-dimensional pendulum. The payload is approximated to be a point mass suspended on a massless, rigid cable which is attached to the trolley via a ball joint. It is assumed that the pendulum exhibits only the fundamental frequency of vibration, with an approximate natural period of

$$T = 2\pi\sqrt{l/g}\,, \tag{1}$$

where g is the acceleration of gravity and l is the pendulum cable length.

The static free-body diagram for a three-dimensional pendulum is shown in Fig. 1, where θ represents the angle of the pendulum with the vertical in the *x-z* plane, and φ represents the angle of the pendulum with the vertical in the *y-z* plane. The *xyz* system translates, but does not rotate with the trolley.

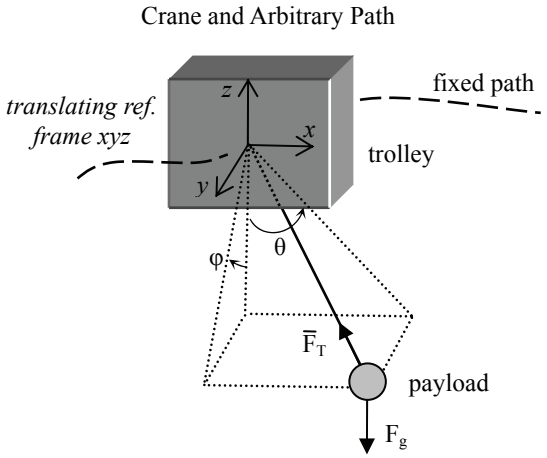

FIGURE 1: DIAGRAM OF CRANE AND PATH

Given the assumptions as stated, the tension force in the cable is equal to the force of gravity component in the cable direction as shown by

$$\left|F_T\right| = F_g\cos(\theta)\cos(\phi)\,. \tag{2}$$

The tension force is decomposed into components in the three coordinate directions by the angle of the pendulum:

$$\begin{aligned}\vec{F}_T\cdot\hat{e}_x &= F_T\cos(\theta)\sin(\phi)\\ \vec{F}_T\cdot\hat{e}_y &= F_T\sin(\theta)\cos(\phi)\,.\\ \vec{F}_T\cdot\hat{e}_z &= F_T\cos(\theta)\cos(\phi)\end{aligned} \tag{3}$$

Expanding the terms from Eq. (3) with Eq. (2) allows the tension force components to be defined in terms of the force of gravity and the angle of the pendulum:

$$\begin{aligned}\vec{F}_T\cdot\hat{e}_x &= F_g\cos(\theta)\cos(\phi)\cos(\theta)\sin(\phi)\\ \vec{F}_T\cdot\hat{e}_y &= F_g\cos(\theta)\cos(\phi)\sin(\theta)\cos(\phi)\,.\\ \vec{F}_T\cdot\hat{e}_z &= F_g\cos(\theta)\cos(\phi)\cos(\theta)\cos(\phi)\end{aligned} \tag{4}$$

The nonlinear system presented in Eq. (4) is linearized by a small angle approximation. The tension force components can

thus be reduced to linear equations in terms of the force of gravity and the pendulum angle,

$$\begin{aligned}\vec{F}_T \cdot \hat{e}_x &= F_g \phi \\ \vec{F}_T \cdot \hat{e}_y &= F_g \theta \\ \vec{F}_T \cdot \hat{e}_z &= F_g\end{aligned} . \quad (5)$$

Since the force of gravity F_g is assumed to be constant, Eqs. (5) are linear and decoupled; thus, the superposition principle can be applied to the vibration calculations of each coordinate direction independently, as done in [6-9] for motion along one dimension.

Vibration is induced in the payload by applied tensile cable forces. The time-varying amplitude of vibration of the crane payload at time t due to an applied pulse force at time $t_i<t$ will be written as $Vt_i(t)$. The subscript indicates the time at which the vibration was induced, while the parenthetical value indicates the time at which the vibration amplitude is evaluated. Then, the total amplitude of time-varying vibration at time t due to all previous pulse forces is equal to the sum of all $Vt_i(t)$ as expressed by

$$\overline{V}(t) = \sum_i \overline{V}t_i(t) . \quad (6)$$

The forces on the pendulum are proportional to its acceleration, which in turn is proportional to the vibration amplitudes. In accordance with the case of a pendulum suspended from a trolley following a curvilinear path, this study will consider acceleration due to two sources: tangential and centripetal acceleration. The resultant acceleration at time t_i is the vector sum of accelerations from these two sources,

$$\overline{a}(t_i) = \overline{a}_c(t_i) + \overline{a}_t(t_i) \propto \overline{V}t_i(t) , \quad (7)$$

and is proportional to the induced vibration at time t_i.

For the purposes of vibration elimination, the proportionality constant between vibration amplitude and accelerations can be absorbed into the vibration amplitude (the units of $Vt_i(t)$ are irrelevant since the sum of the time-varying amplitudes of vibration will eventually be driven to zero). Other sources of acceleration, such as Coriolis effects, are assumed to be negligible. By incorporating Eq. (7) with Eq. (6), the time-varying amplitude of vibration at time t can be expressed as the sum of current accelerations and vibrations induced at previous times (i.e. the vibration accumulates):

$$\begin{aligned}&\overline{V}(0) = \overline{a}_c(0) + \overline{a}_t(0) = \overline{V}_0(0) \\ &\overline{V}(\delta t) = \overline{V}_0(\delta t) + \overline{a}_c(\delta t) + \overline{a}_t(\delta t) = \overline{V}_0(\delta t) + \overline{V}_{\delta t}(\delta t) \\ &\overline{V}(2\delta t) = \overline{V}_0(2\delta t) + \overline{V}_{\delta t}(2\delta t) + \overline{a}_c(2\delta t) + \overline{a}_t(2\delta t) \\ &\vdots\end{aligned} , \quad (8)$$

where δt denotes an infinitesimal time step.

The goal of this research is to cause the amplitude of vibration to go to zero at the stopping position and time of the path-constrained trolley. In the next section, two command shapers will be developed to achieve this.

DEVELOPMENT OF GENERALIZED CONSTRAINED PATH COMMAND SHAPERS

To drive induced vibrations to zero, command shaping techniques are invoked. Here, the generalized CTV shaper is developed first to account for both centripetal and tangential accelerations. Then, the simplified TV shaper is developed accounting for only tangential accelerations.

Development of CTV Shaper

Vibrations that are induced at times $t+a$T (for integer a) sum, causing the vibration amplitude to increase, and vibrations that are induced at times $t+a$T/2 cancel (ref. Fig. 3b). The vector quantities in Eq. (8) are decomposed into scalar quantities in the x and y directions, then—according to the command shaping method—the vibrations induced at each multiple of half-period times are required to cancel, giving

$$\begin{aligned}&\sum_{j=0,2,\ldots}^{n} V_x\left(j\tfrac{T}{2}\right)(t) - \sum_{j=1,3,\ldots}^{n} V_x\left(j\tfrac{T}{2}\right)(t) = 0 \\ &\sum_{j=0,2,\ldots}^{n} V_x\left(\delta t + j\tfrac{T}{2}\right)(t) - \sum_{j=1,3,\ldots}^{n} V_x\left(\delta t + j\tfrac{T}{2}\right)(t) = 0 \\ &\vdots \\ &\sum_{j=0,2,\ldots}^{n} V_x\left(m\delta t + j\tfrac{T}{2}\right)(t) - \sum_{j=1,3,\ldots}^{n} V_x\left(m\delta t + j\tfrac{T}{2}\right)(t) = 0\end{aligned} \quad (9a)$$

$$\begin{aligned}&\sum_{j=0,2,\ldots}^{n} V_y\left(j\tfrac{T}{2}\right)(t) - \sum_{j=1,3,\ldots}^{n} V_y\left(j\tfrac{T}{2}\right)(t) = 0 \\ &\sum_{j=0,2,\ldots}^{n} V_y\left(\delta t + j\tfrac{T}{2}\right)(t) - \sum_{j=1,3,\ldots}^{n} V_y\left(\delta t + j\tfrac{T}{2}\right)(t) = 0 \\ &\vdots \\ &\sum_{j=0,2,\ldots}^{n} V_y\left(m\delta t + j\tfrac{T}{2}\right)(t) - \sum_{j=1,3,\ldots}^{n} V_y\left(m\delta t + j\tfrac{T}{2}\right)(t) = 0\end{aligned} . \quad (9b)$$

In Eqs. (9), m and n are defined as

$$n = \left\lfloor \frac{t_f}{T/2} \right\rfloor , \quad m = \frac{T/2}{\delta t} , \quad (10)$$

where t_f is the move time for the trolley, and $\lfloor\rfloor$ denotes the floor function. For example, if the trolley must come to rest by time t=3T, then n=6. The value of m will depend on resolution of the discretization, δt.

To determine the impulse magnitudes and times necessary to drive vibration to zero, Eqs. (9) must be expanded in terms of the trolley accelerations, which requires $\boldsymbol{a_c}$ and $\boldsymbol{a_t}$ in Fig. 2 to be resolved into x- and y-components. To accomplish this, define the angle Ψ as the angle between the x-direction and a vector between point s and the center of the osculating circle at point s as shown in Fig. 2. Observe that in general, Ψ is a function of time and path geometry: $\Psi = \Psi(s(t))$.

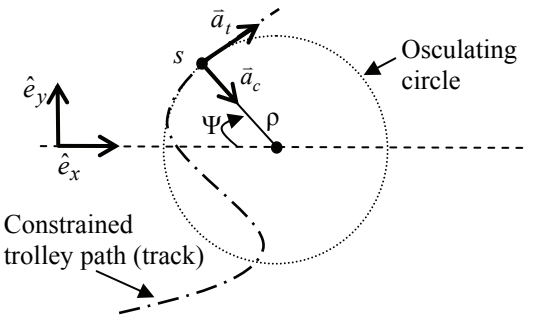

FIGURE 2: RADIUS OF CURVATURE AND ANGLE FOR ANY POINT ALONG THE CONSTRAINED TROLLEY PATH

With this definition, Eqs. (9) are expressed in terms of trolley accelerations $a_c(t)$ and $a_t(t)$, yielding:

$$\begin{aligned}
&\sum_{j=0,2,\ldots}^{n}\left(\left(\vec{a}_c(t)+\vec{a}_t(t)\right|_{t=j\frac{T}{2}}\right)\cdot\hat{e}_x-\sum_{j=1,3,\ldots}^{n}\left(\left(\vec{a}_c(t)+\vec{a}_t(t)\right|_{t=j\frac{T}{2}}\right)\cdot\hat{e}_x=0\\
&\sum_{j=0,2,\ldots}^{n}\left(\left(\vec{a}_c(t)+\vec{a}_t(t)\right|_{t=\delta t+j\frac{T}{2}}\right)\cdot\hat{e}_x-\sum_{j=1,3,\ldots}^{n}\left(\left(\vec{a}_c(t)+\vec{a}_t(t)\right|_{t=\delta t+j\frac{T}{2}}\right)\cdot\hat{e}_x=0\\
&\quad\vdots\\
&\sum_{j=0,2,\ldots}^{n}\left(\left(\vec{a}_c(t)+\vec{a}_t(t)\right|_{t=m\delta t+j\frac{T}{2}}\right)\cdot\hat{e}_x-\sum_{j=1,3,\ldots}^{n}\left(\left(\vec{a}_c(t)+\vec{a}_t(t)\right|_{t=m\delta t+j\frac{T}{2}}\right)\cdot\hat{e}_x=0
\end{aligned}\tag{11a}$$

$$\begin{aligned}
&\sum_{j=0,2,\ldots}^{n}\left(\left(\vec{a}_c(t)+\vec{a}_t(t)\right|_{t=j\frac{T}{2}}\right)\cdot\hat{e}_y-\sum_{j=1,3,\ldots}^{n}\left(\left(\vec{a}_c(t)+\vec{a}_t(t)\right|_{t=j\frac{T}{2}}\right)\cdot\hat{e}_y=0\\
&\sum_{j=0,2,\ldots}^{n}\left(\left(\vec{a}_c(t)+\vec{a}_t(t)\right|_{t=\delta t+j\frac{T}{2}}\right)\cdot\hat{e}_y-\sum_{j=1,3,\ldots}^{n}\left(\left(\vec{a}_c(t)+\vec{a}_t(t)\right|_{t=\delta t+j\frac{T}{2}}\right)\cdot\hat{e}_y=0\\
&\quad\vdots\\
&\sum_{j=0,2,\ldots}^{n}\left(\left(\vec{a}_c(t)+\vec{a}_t(t)\right|_{t=m\delta t+j\frac{T}{2}}\right)\cdot\hat{e}_y-\sum_{j=1,3,\ldots}^{n}\left(\left(\vec{a}_c(t)+\vec{a}_t(t)\right|_{t=m\delta t+j\frac{T}{2}}\right)\cdot\hat{e}_y=0
\end{aligned}\tag{11b}$$

Equations (11) are constraint equations that must be satisfied to yield zero payload vibration at the stopping time t_f. Observe that the dot products are a function of Ψ, which itself is a function of path geometry and time. In the development of the CTV shaper, centripetal effects are considered. The centripetal acceleration of the payload is modeled as

$$a_c(t)=\frac{v(t)^2}{\rho(s)},\tag{12}$$

where $\rho(s)$ is the radius of curvature of the path and $v(t)$ is the velocity of the trolley. Note that it is assumed the velocity and path of the crane payload is equal to the velocity and path of the trolley because a small angle approximation was made. The velocity term in Eq. (12) is a function of the acceleration along the path, as given by

$$v(t)=\int_0^t a_t(t)dt\ .\tag{13}$$

Because the equations for the shaper have been derived in discrete time, Eq. (13) can also be written as a discrete sum. At any instant, induced vibration is proportional to the net acceleration which is a function of velocity and $\rho(s(t))$; consequently, there is vibration induced at each infinitesimal time step δt as shown in Fig. 3a. For the continuously induced vibration to cancel, it is necessary that vibration induced in phase (i.e. induced at time multiples of T) cancel with vibration out of phase (i.e. induced at time multiples of T/2) as indicated in Eqs. (12,13) and in Fig. 3b.

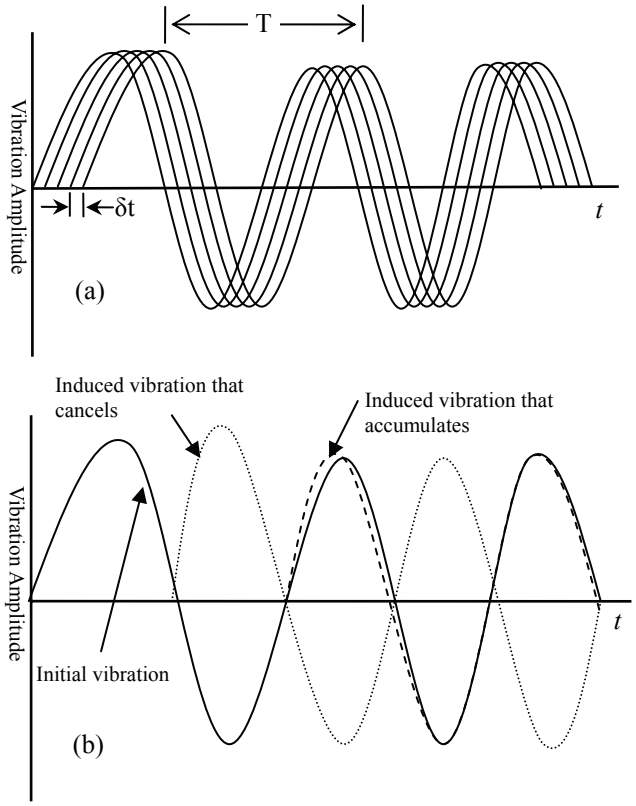

FIGURE 3: (a) DISCRETIZED CONTINUOUSLY INDUCED CENTRIPETAL VIBRATION. (b) ILLUSTRATION OF THE ADDING AND CANCELING OF VIBRATIONS IN AND OUT OF PHASE

For positioning the crane, the reference velocity profile, $v_R(t)$, is convolved with $A(t)$, the designed command shaper, to give the shaped velocity profile; differentiation of this shaped velocity profile yields the trolley acceleration along the path, as shown by

$$v_S(t)=v_R(t)*A(t)\ \text{ and}\tag{14}$$

$$a_t(t)=\dot{v}_S(t)\tag{15}$$

where * is the convolution operator and an over dot denotes time differentiation. Fig. 4 illustrates the process of determining a_t from v_R.

This paper assumes the approximation that the crane can exactly follow the shaped velocity profile (so that $a_t(t)$ equals the actual trolley tangential acceleration); otherwise the crane dynamics must be considered.

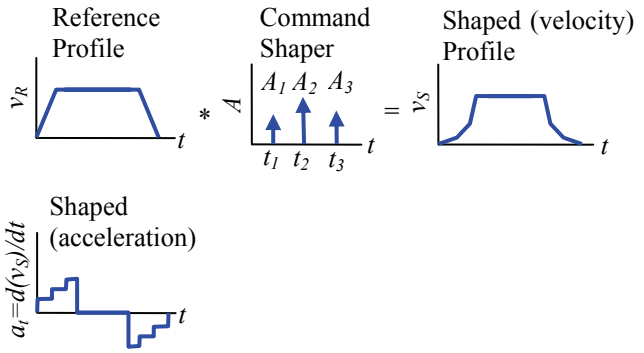

FIGURE 4: DETERMING SHAPED VELOCITY AND ACCELERATION ALONG THE PATH FROM CONVOLUTION

The impulse magnitudes and times for the CTV shaper, *A(t)* in Eq. (14), are solved for numerically such that the zero-vibration constraints of Eqs. (11) are satisfied), then normalized by the sum of accelerations as shown in Eq. (16) to give the amplitudes of the CTV shaper.

$$A(t) = a_t(t)\left(\sum_{\tau=0,\delta t,2\delta t,\cdots}^{t_f} a_t(\tau)\right)^{-1} \tag{16}$$

Notice that, in general, there are many solutions for the under-constrained Eqs. (11). Next, a simplification is made to Eqs. (11) to develop the simplified TV shaper, and a method of solving these equations is presented.

Development of TV Command Shaper

In this sub-section, the TV shaper is developed by considering centripetal effects to be negligible. Centripetal effects can also be eliminated, and Eqs. (11) verified, by considering the trolley to be constrained to follow a straight line. In this sub-section, the straight-line simplification is presented, then the TV shaper for a curvilinear path is developed.

Straight-Line Verification of Shaper Equations The TV and CTV shaper methods can be verified by comparing a straight-line simplification of Eqs. (11) with the well-known ZV command shaper [5-7]. For a straight-line path

$$a_c(t) = 0, \text{and } \Psi(t) = 0\,. \tag{17}$$

Eqs. (17) are substituted into Eqs. (11) to obtain

$$\begin{aligned} &a_t(0) - a_t\left(\frac{T}{2}\right) + a_t(T) - a_t\left(\frac{3T}{2}\right)\ldots = 0 \\ &a_t(\delta t) - a_t\left(\delta t + \frac{T}{2}\right) + a_t(\delta t + T) - a_t\left(\delta t + \frac{3T}{2}\right)\ldots = 0\,. \\ &\vdots \end{aligned} \tag{18}$$

Normalization of Eqs. (18) by Eq. (16) results in a description of all possible shapers. There are many solutions to this under-constrained problem; however, to determine the simplest and quickest shaper, Eqs. (18) are solved by setting as many terms as possible to zero, with the nonzero terms occurring as early as possible. It is known that $a_t(0) \neq 0$, so it is not possible to set *all* terms in the first equation of Eqs. (18) to zero, but the first equation *can* be solved with only one nonzero term:

$$a_t(0) = a_t\left(\frac{T}{2}\right). \tag{19}$$

All other terms can be set to zero to satisfy all equations in Eqs. (18). Normalizing Eq. (19) according to Eq. (16) defines a shaper with equal impulses at times 0 and T/2. Thus the CTV shaper for linear motion is the well-known ZV shaper discussed in [5-7].

Development of TV Shaper for Constrained Curvilinear Path. This section will show that at least three impulses are required to eliminate payload vibration induced along a curvilinear path. The TV shaper is designed to minimize payload vibrations induced by accelerations along the tangential direction of the constrained curvilinear trolley path. The TV shaper is derived by aligning *x*-axis with the radial direction at the beginning of the path and neglecting centripetal effects (after assuming $(v_l)^2/\rho \ll 1$), giving

$$a_c(t) = 0 \text{ and } \Psi(0) = 0\,. \tag{20}$$

Using Eq. (20), the CTV constraints in Eqs. (11) simplify to

$$\begin{aligned} &\sum_{j=0,2,\ldots}^{n} a_t\left(j\frac{T}{2}\right)\sin\left(\Psi\left(j\frac{T}{2}\right)\right) - \sum_{j=1,3,\ldots}^{n} a_t\left(j\frac{T}{2}\right)\sin\left(\Psi\left(j\frac{T}{2}\right)\right) = 0 \\ &\sum_{j=0,2,\ldots}^{n} a_t\left(\delta t + j\frac{T}{2}\right)\sin\left(\Psi\left(\delta t + j\frac{T}{2}\right)\right) - \sum_{j=1,3,\ldots}^{n} a_t\left(\delta t + j\frac{T}{2}\right)\sin\left(\Psi\left(\delta t + j\frac{T}{2}\right)\right) = 0 \\ &\vdots \\ &\sum_{j=0,2,\ldots}^{n} a_t\left(m\delta t + j\frac{T}{2}\right)\sin\left(\Psi\left(m\delta t + j\frac{T}{2}\right)\right) - \sum_{j=1,3,\ldots}^{n} a_t\left(m\delta t + j\frac{T}{2}\right)\sin\left(\Psi\left(m\delta t + j\frac{T}{2}\right)\right) = 0 \end{aligned} \tag{21a}$$

$$\begin{aligned} &\sum_{j=0,2,\ldots}^{n} a_t\left(j\frac{T}{2}\right)\cos\left(\Psi\left(j\frac{T}{2}\right)\right) - \sum_{j=1,3,\ldots}^{n} a_t\left(j\frac{T}{2}\right)\cos\left(\Psi\left(j\frac{T}{2}\right)\right) = 0 \\ &\sum_{j=0,2,\ldots}^{n} a_t\left(\delta t + j\frac{T}{2}\right)\cos\left(\Psi\left(\delta t + j\frac{T}{2}\right)\right) - \sum_{j=1,3,\ldots}^{n} a_t\left(\delta t + j\frac{T}{2}\right)\cos\left(\Psi\left(\delta t + j\frac{T}{2}\right)\right) = 0 \\ &\vdots \\ &\sum_{j=0,2,\ldots}^{n} a_t\left(m\delta t + j\frac{T}{2}\right)\cos\left(\Psi\left(m\delta t + j\frac{T}{2}\right)\right) - \sum_{j=1,3,\ldots}^{n} a_t\left(m\delta t + j\frac{T}{2}\right)\cos\left(\Psi\left(m\delta t + j\frac{T}{2}\right)\right) = 0 \end{aligned} \tag{21b}$$

For the derivation of the TV shaper presented in this paper, assume that tangential acceleration is caused by impulses occurring over a negligible time span (i.e. the crane actuators have negligible dynamic effects). As before, the desired solution should have a minimum number of impulses occurring at the earliest possible times. The only term in Eqs. (21) that is initially guaranteed to be nonzero is $a_t(0)$, so the simplest form of the first equation of (21b) is solved by keeping only *j=0,1* to give

$$a_t(0) = a_t\left(\frac{T}{2}\right)\cos\left(\Psi\left(\frac{T}{2}\right)\right), \tag{22}$$

suggesting that $a_t(T/2) \neq 0$. Because this term also appears in the first equation of (21a), another constraint using only $j=1,2$ is

$$a_t\left(\frac{T}{2}\right)\sin\left(\Psi\left(\frac{T}{2}\right)\right) = a_t(T)\sin\left(\Psi(T)\right), \qquad (23)$$

which suggests that $a_t(T) \neq 0$; thus, the other parts of Eq. (21) having $a_t(T)$ need to be considered. Additionally, Eq. (22) no longer holds, because (23) required that terms up to $j=2$ be kept. Hence, Eq. (23) is amended with this additional term giving

$$a_t(0) - a_t\left(\frac{T}{2}\right)\cos\left(\Psi\left(\frac{T}{2}\right)\right) + a_t(T)\cos\left(\Psi(T)\right) = 0\,. \qquad (24)$$

Eqs. (23,24), along with the normalization requirement Eq. (16), give three equations for the three unknown impulse amplitudes $A(0), A(\frac{T}{2}), A(T)$, which are then convolved with the reference profile to produce the shaped profile needed for no payload vibration. Observe that when solving for the TV shaper, it is not required to know the reference profile in advance, as it was for the CTV shaper.

Eqs. (23,24) show that at least three impulses are necessary to achieve zero vibration when accounting only for tangential accelerations along a constrained generalized curvilinear path.

Fig. 5 illustrates the TV shaper, in which three impulses A_1, A_2, A_3 accelerate the trolley along the curved path.

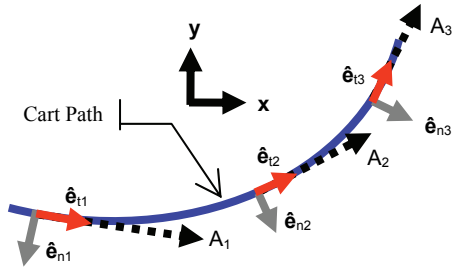

FIGURE 5: ILLUSTRATION OF 3-IMPULSE SEQUENCE USED TO ACCELERATE TROLLEY ALONG PATH

EXPERIMENTAL RESULTS FROM MODEL CRANE

This section presents the results of implementing the CTV and TV shapers on an actual miniature crane constrained to follow a circular path. The benefits of the shapers will be quantified and the robustness of the shapers evaluated.

The CTV and TV shapers were applied to a model bridge crane in the Advanced Crane Controls Laboratory at the Georgia Institute of Technology [15]. The trolley of the mini bridge crane was constrained to traverse 90-degrees of a circular path of radius R=25 cm. The payload was suspended with a nominal cable length of 55 cm.

A *Siemens AG* PLC motion control system drives the two axes of the bridge crane. The PLC was programmed to always accelerate the trolley linearly in time to a given velocity in 0.5 seconds. Thus, for this application, the tangential acceleration is modeled as either zero or--during periods of acceleration--as

$$a_{t_x}(\tau) = a_{t_x}(\tau + 0.5) = \frac{v(\tau+0.5) - v(\tau)}{0.5}\cos(\theta(t)) \qquad (25a)$$

$$a_{t_y}(\tau) = a_{t_y}(\tau + 0.5) = \frac{v(\tau+0.5) - v(\tau)}{0.5}\sin(\theta(t)), \qquad (25b)$$

where τ is the acceleration start time.

The crane is moved with three acceleration pulses at times 0, T/2, and T, and three deceleration pulses at aT/2, (a+1)T/2, and (a+2)T/2 where a is an integer. Let the velocity at time T/2 be v_1, the velocity at time T be v_2, and the velocity at time aT/2 be v_3. Then to decelerate, the velocity at time (a+1)T/2 is v_2, at time (a+2)T/2 is v_1, and at time (a+2)T/2+0.5 and beyond is 0. Notice that the stopping time must be integer multiples of half the natural payload period.

Substituting (25) into (11) and imposing that the only nonzero tangential accelerations occur at the chosen impulse times give the necessary constraint equations for the CTV shaper:

$$\sum_{j=0}^{n}\left(\frac{v(\Delta(j)+0.5)-v(\Delta(j))}{0.5}\cos(\theta(\Delta(j)))\right)+\frac{v^2(\Delta(j))}{r}\cos(\theta(\Delta(j))) \qquad (26a)$$
$$=\sum_{j=0}^{n}\left(\frac{v(\Delta(j)+\frac{T}{2}+0.5)-v(\Delta(j)+\frac{T}{2})}{0.5}\cos\left(\theta(\Delta(j)+\frac{T}{2})\right)\right)+\frac{v^2(\Delta(j)+\frac{T}{2})}{r}\cos(\theta(\Delta(j)+\frac{T}{2}))$$

$$\sum_{j=0}^{n}\left(\frac{v(\Delta(j)+0.5t)-v(\Delta(j))}{0.5}\sin(\theta(\Delta(j)))\right)+\frac{v^2(\Delta(j))}{r}\sin(\theta(\Delta(j))) \qquad (26b)$$
$$=\sum_{j=0}^{n}\left(\frac{v(\Delta(j)+\frac{T}{2}+0.5)-v(\Delta(j)+\frac{T}{2})}{0.5}\sin\left(\theta(\Delta(j)+\frac{T}{2})\right)\right)+\frac{v^2(\Delta(j)+\frac{T}{2})}{r}\sin(\theta(\Delta(j)+\frac{T}{2}))$$
$$\Delta(j) \equiv jT + k\delta t$$

The impulse amplitudes for the CTV shaper are found by solving Eq. (14) for $A(t)$, subject to the constraints of Eqs. (26).

The impulse amplitudes for the TV shaper are found by solving Eqs. (23,24) and Eq. (16) for the impulse amplitudes.

The normalized impulse magnitudes and times for the TV shaper implementation was calculated to be as shown in Eq. (27), and the solution for the CTV shaper is shown in Eq. (28).

$$\begin{bmatrix} A_i \\ t_i \end{bmatrix} = \begin{bmatrix} 0.426 & 0.431 & 0.143 \\ 0 & 0.5T & T \end{bmatrix} \text{(TV)} \qquad (27)$$

$$\begin{bmatrix} A_i \\ t_i \end{bmatrix} = \begin{bmatrix} 0.290 & 0.500 & 0.210 \\ 0 & 0.5T & T \end{bmatrix} \text{(CTV)} \qquad (28)$$

In this example the commanded speed along the trolley path is a step of magnitude v_{max}=0.14 m/s. This tangential speed command is convolved with the designed shapers.

Three test cases were run on the model crane: TV shaper implementation, CTV shaper implementation, and unshaped movement. In each case, the inverse shaper was used to

decelerate the trolley. The actual recorded trolley path for all experiments is shown in Fig. 6.

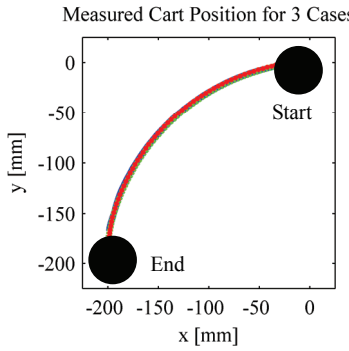

FIGURE 6: CART POSITION FOR EACH EXPERIMENT

Fig. 7 shows the measured velocity in the direction tangent to the constrained path for the three different shapers (TV, CTV, and unshaped). The measured velocity perpendicular to the path was verified to be zero, thus satisfying the imposed path constraint. Observe that Fig. 7 highlights an artifact often encountered with command shaping: a shaped input command generally takes longer to execute than the original (unshaped) command, thereby introducing a move-time penalty that must be considered when designing the positioning system.

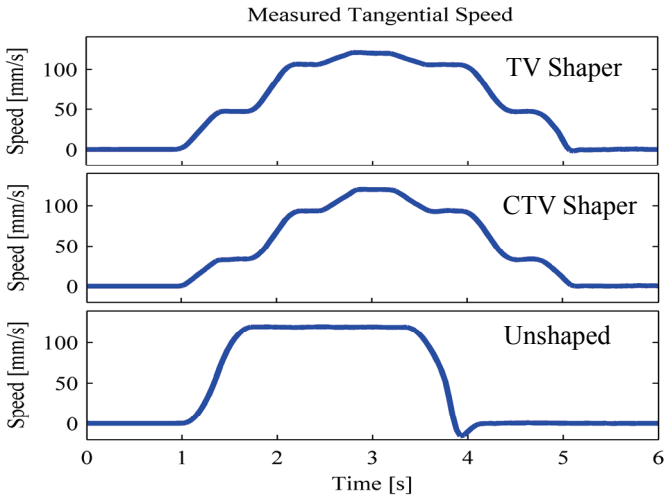

FIGURE 7: MEASURED SPEED ALONG PATH

Fig. 8 shows a plot of the payload position during movement, as recorded by an overhead camera mounted on the trolley. Notice that of the three test cases, the CTV shaper causes the payload to sway the least during the point-to-point movement of the trolley. When the trolley stops moving, the residual payload vibration traces an ellipse. Fig. 9 is a comparison of the residual payload vibration projected along the major axis of the ellipse traced by the payload after the trolley has come to rest at its final position. The CTV shaper has marginally less swing magnitude than the TV shaper in this case.

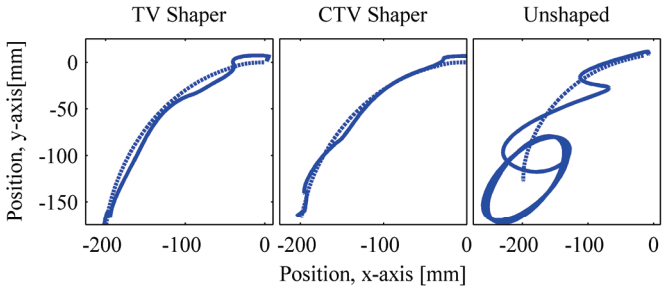

FIGURE 8: MEASURED POSITION OF TROLLEY (DASHED LINES) AND PAYLOAD (SOLID) FOR THE THREE CASES

Fig. 9 indicates that the vibration resulting from unshaped point-to-point motion is 160 mm peak-to-peak. Both the CTV and TV shaper reduce the vibration to approximately 7% of the unshaped amplitude.

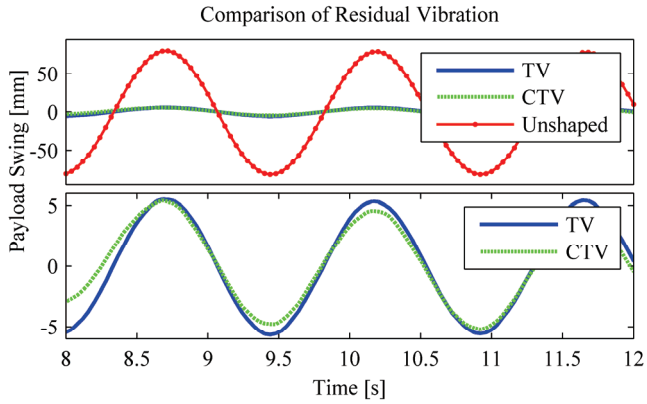

FIGURE 9: COMPARISON OF RESIDUAL VIBRATION FOR THE THREE CASES

Sensitivity Analysis of Shapers

Experiments were performed on the model crane to test the robustness of the CTV shaper to modeling errors. Three types of modeling errors were tested: errors in path radius specification, errors in natural frequency calculation (i.e. the payload is hoisted to a height different from the designed height), and errors in system type.

The sensitivity curves in Fig. 10 highlight the robustness of the command shaper [11]. The abscissa of Fig. 10a gives the normalized frequency, defined as the actual system frequency divided by the modeled frequency. The ordinate shows the normalized residual vibration magnitude, defined as the sum of the payload vibration amplitudes projected along the major and minor axes of the ellipse traced during the residual vibration.

The sensitivity curve for natural frequency (Fig. 10a) indicates that the shaper is relatively insensitive to modeling errors near the nominal value, but the performance degrades rapidly when the error is larger than 40%. When the actual path radius is much smaller than the radius used for designing the shaper, the residual vibration tends to increase, as in Fig. 9b, because the smaller radius results in higher centripetal

acceleration inducing components of payload swing larger than the command shaper is designed to account for.

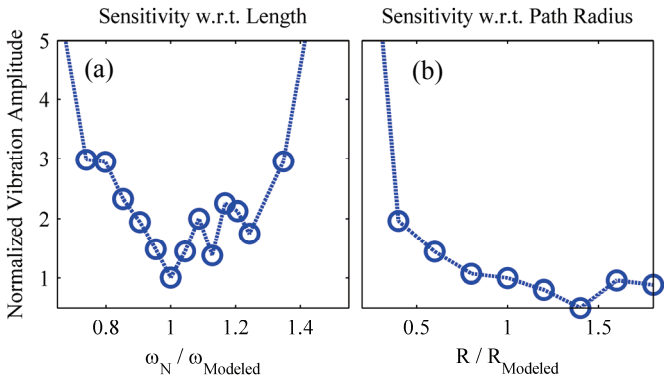

FIGURE 10: SENSITIVITY CURVES FOR ERRORS IN PATH RADIUS AND PENDULUM LENGTH

Fig. 11 shows the residual vibration resulting from using a single-mode shaper on a double-mode (double pendulum) system. In this case, the double-mode system was a payload mass hanging approximately 10 cm from the crane's hook. The payload mass was about 10 times the crane's hook mass. The hook's length of 55 cm was used to design the impulse amplitudes of the shaper. Notice that only a marginal amount of additional vibration is induced in this double-mode system when compared with Fig. 9 for a single mode system, illustrating that the shaper is robust to modeling errors in the order of the system.

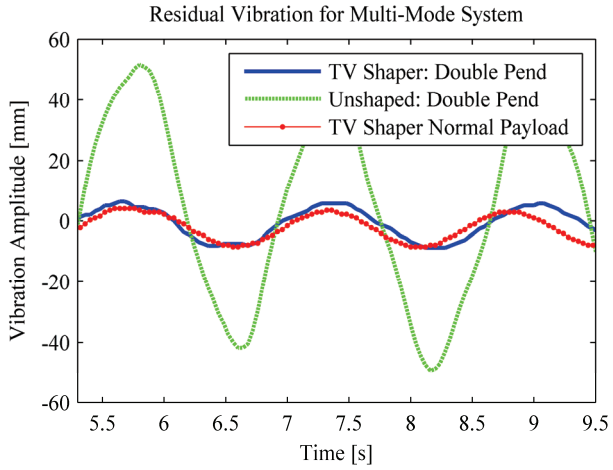

FIGURE 11: RESIDUAL VIBRATION FOR ERRORS IN SYSTEM TYPE: SINGLE MODE SHAPER USED ON DOUBLE MODE SYSTEM

DISCUSSION

While the TV shaper allows for any arbitrary stop time, the stop time for the CTV shaper must occur at integer multiples of half-periods in order to sufficiently cancel the continuously-induced vibration from centripetal effects. This stop time must be known when solving the CTV shaper equations.

Because of the continuously-induced nature of centripetal acceleration, for an exact solution of the CTV shaper in Eqs. (11), an infinite number of constraint equations must be satisfied simultaneously. However, this work has shown that the equations can be discretized in time and a satisfactory solution can be found by solving one equation for each time step. Because tangential acceleration is not continuous, the TV shaper has a simpler solution that requires only three impulses, as indicated in Eqs. (23,24) and Fig. 5.

In the implementation of the two shapers, the CTV shaper proved to be only a slight improvement over the simplified TV shaper, indicating that centripetal effects in the tested case are minor. Additionally, in this case the TV shaper is slightly faster than the CTV shaper by about 0.5 sec, as indicated in Fig. 7 and the unshaped motion is slightly faster than the TV shaper. For these reasons, the TV shaper may be more useful that the CTV shaper in cases where speed of response is critical.

The CTV shaper was also tested with modeling errors to determine the robustness. From the results displayed in Fig. 10, the CTV shaper was found to be relatively insensitive to modeling errors in path radius. For example, if a shaper designed for a certain radius (in this study, R=25 cm) is used to move the trolley along a path of larger or slightly smaller radius, then the residual vibration will remain at an acceptable level. However, if the actual radius is less than about 60 % of the modeled radius then vibration increases significantly, as shown in Fig. 10. The CTV shaper is more sensitive to decreases in radius because the unmodeled component of the centripetal acceleration is inversely proportional to the radius. The CTV shaper has a similar sensitivity to natural frequency modeling errors as other 3-impulse shapers [11].

A possible future extension of this study is to account for Coriolis effects and other inherently nonlinear aspects of the crane and pendulum system. The shaper designed to account for these nonlinearities could then be compared to the TV and CTV shapers to determine the impact of the nonlinear effects. Further comparisons should be made between these shapers and other types of command pre-filtering, such as S-curve acceleration profiles. Also, the CTV and TV shapers should be experimentally verified with other path geometries.

CONCLUSIONS

Two command shapers were developed to cancel vibration of a payload suspended from a trolley constrained to follow a specified curvilinear path. The designed CTV shaper cancels vibration induced by both tangential and centripetal accelerations, while the TV shaper cancels only tangentially induced vibrations. It was determined that the TV shaper can be implemented with three impulses occurring at times 0, T/2, and T. It was also determined that in order to cancel centripetal acceleration-induced vibration with the CTV shaper, the stop time must be an integer multiple of T/2.

Both shapers were tested experimentally on a model crane constrained to follow a circular path. Experimentally, the peak-to-peak vibration of the unshaped system was 160 mm. The TV shaper resulted in a peak-to-peak vibration of less than 12 mm, or about 7% of the unshaped vibration.

The shapers were found to be robust to modeling errors in both natural frequency and radius. Both the TV and CTV

shapers can be highly effective at canceling out residual vibration in this constrained path problem.

ACKNOWLEDGMENTS

The authors would like to thank Siemens Energy and Automation for their support of this work. The authors would also like to thank Dr. William Singhose for his instruction and assistance with this project.

REFERENCES

[1] Abdel-Rahman, E., Nayfeh, A., and Masoud, Z., 2003, "Dynamics and Control of Cranes: A Review," J. of Vibration and Control, 9, pp. 863-908.

[2] Lee, H., 2004, "A New Design Approach for the Anti-Swing Trajectory Control of Overhead Cranes with High-Speed Hoisting," International J. of Control, 77(10), pp. 931-940.

[3] Lew, J., Khalil, A., 2000, "Anti-Swing Control of a Suspended Load with a Robotic Crane," Proc. of the American Control Conference, 2, Phoenix, Arizona, pp. 1042-1046.

[4] Yi, J., Yubazaki, N., and Hirota, K., 2003, "Anti-swing and positioning control of overhead traveling crane," Information Sciences: an International Journal, 155(1-2), pp. 19-42.

[5] Smith, O. J. M., 1957, "Posicast Control of Damped Oscillatory Systems", Proc. of the IRE, pp 1249-1255.

[6] Singer, N., and Seering, W., 1990, "Preshaping command inputs to reduce system vibration," J. of Dynamic Sys., Measurement, and Control, 112, pp. 76-82.

[7] Garrido, S., Abderrahim, M., Giménez, A., and Balaguer, C., 2003, "Antiswinging Input Shaping Control of an Automatic Construction Crane", *The 11th Mediterranean Conf. On Control and Automation*. Rodas. Greece.

[8] Singhose, W., Seering, W., and Singer., N, 1994, "Residual Vibration Reduction using Vector Diagrams to Generate Shaped Inputs," J. Dyn. Sys. Meas. & Control, 116(2), pp. 654-659.

[9] Yun, J., Park., B, Lee, J., Park, H., 1996, "Velocity Control Method for Preventing Oscillations in Crane," United States Patent, No. 5,550,733.

[10] Singer, N., Singhose, W., and Kriikku, E., 1997, "An Input Shaping Controller Enabling Cranes to Move Without Sway," American Nuclear Society 7th Topical Meeting on Robotics and Remote Systems, Augusta, Georgia.

[11] Singh T., and Singhose, W., 2002, "Tutorial on Input Shaping/Time Delay Control of Maneuvering Flexible Structures", 2002 American Control Conference, May 8-10, Anchorage, Alaska.

[12] Lawrence, J., 2006, "Crane Oscillation Control: Nonlinear Elements and Educational Improvements," Ph.D. Dissertation, Georgia Institute of Technology, Atlanta, Georgia.

[13] Singhose, W., and Singer, N., 1996, "Effects of Input Shaping on Two-Dimensional Trajectory Following," IEEE Trans. on Robotics and Automation, 12(6), pp. 881-87.

[14] Blackburn, D., Singhose, W., Kitchen, J., Patrangenaru, V., Lawrence, J., Kamoi, T., and Taura, A., 2006, "Advanced Input Shaping Algorithm for Nonlinear Tower Crane Dynamics," Int. Conf. on Motion and Vibration Control, Daejeon, Korea.

[15] J. Lawrence and W. Singhose, 2005, "Design of Minicrane for Education and Research," 6th Int. Conference on Research and Education in Mechatronics, Annecy, France.